Available online at www.sciencedirect.com
ScienceDirect
Colloids and Surfaces A: Physicochem. Eng. Aspects 290 (2006) 7–18
COLLOIDS AND SURFACES A
www.elsevier.com/locate/colsurfa

Zinc basic benzoate as eco-friendly steel corrosion inhibitor pigment for anticorrosive epoxy-coatings

G. Blustein, R. Romagnoli, J.A. Jaén, A.R. Di Sarli, B. del Amo *

CIDEPINT—Centro de Investigación y Desarrollo en Tecnología de Pinturas, Calle 52e/121 y 122, B1900AYB La Plata, Argentina

Received 10 January 2006; received in revised form 11 April 2006; accepted 25 April 2006
Available online 5 May 2006

Abstract

The inhibitive properties of benzoate anion were known from many years ago but the employment of soluble compounds in anticorrosive paints is limited because their lixiviation would greatly increase coating permeability. However, it is possible to prepare insoluble metallic benzoates with certain cations. This paper describes the experimental procedure to prepare zinc basic benzoate to be employed in anticorrosive paints. The anticorrosive properties of zinc basic benzoate were assessed by electrochemical techniques (corrosion potential and linear polarization measurements). The nature of the compounds forming the protective layer was determined by different techniques, including spectroscopic ones. In a second stage, the anticorrosive properties of the pigment were evaluated by incorporating it in epoxy anticorrosive paints which, in turn, were evaluated by accelerated (salt spray and humidity tests) and electrochemical measurements (electrochemical impedance spectroscopy). The morphology and the nature of the protective layer grown under the paint film in the salt spray chamber was assessed by scanning electron microscopy (SEM) and UV–vis diffuse reflectance spectroscopy.

Experimental results showed that basic zinc benzoate was adequate to formulate epoxy anticorrosive paints with improved anticorrosive performance, especially with the water-borne binder.
© 2006 Elsevier B.V. All rights reserved.

Keywords: Anticorrosive coatings; Zinc basic benzoate; Accelerated tests; Electrochemical tests

1. Introduction

The inhibitive properties of benzoate anion were known from many years ago and were studied employing sodium benzoate and benzoic acid, in different media, still those containing chloride [1–15]. The employment of benzoate anion in combination with other anions such as gluconates was also reported [16] and, more recently, the inhibitive properties of calcium benzoate in neutral media were described [17]. Sodium benzoate and benzoic acid were used as corrosion inhibitors not only for ferrous substrates but also for other metals such as aluminium [18–22], zinc [23,24] and copper [25]. The mechanism of the anticorrosive action of benzoates involves the adsorption of the anion on the active sites of the metallic surface, thus yielding to an effective coverage which causes the corrosion rate to decrease [16,26,27].

Soluble salts of benzoic acid were also employed in concrete [28,29] and in the field of paint technology. In this last case, they were used as soluble inhibitive additives in anticorrosive coatings and as active insoluble pigments in antifouling paints [30–38].

The employment of soluble compounds (benzoic acid, sodium benzoate, etc.) in anticorrosive paints is limited by the fact that their lixiviation by water penetrating the pores of the coating would greatly increase its permeability with the concomitant loss of the protective properties of the paint. However, it is possible to prepare insoluble metallic benzoates with certain cations (zinc, iron, aluminium, etc.) whose compounds are widely used in paint technology. In addition, zinc salts have recognized inhibitive properties due to the cation which may polarize cathodic areas by the precipitation of sparingly soluble salts and by increasing the pH of the medium, thus favouring steel passivation [39,40].

The objective of this investigation was to study the inhibitive properties of zinc basic benzoate in paints. The pigment was precipitated under definite conditions and its anticorrosive prop-

* Corresponding author. Tel.: +54 221 4831141/44; fax: +54 221 4271537.
E-mail address: pintprotec2@cidepint.gov.ar (B. del Amo).

0927-7757/$ – see front matter © 2006 Elsevier B.V. All rights reserved.
doi:10.1016/j.colsurfa.2006.04.043

erties were investigated by means of electrochemical techniques in pigment suspensions. In a second stage, anticorrosive paints containing zinc basic benzoate were formulated and their performance was evaluated by accelerated (salt spray and humidity chambers) and electrochemical (EIS) tests.

2. Experimental

2.1. Pigment preparation and characterisation

The solution-precipitate equilibrium between zinc cation and benzoate anion was studied in order to find the most suitable conditions to precipitate zinc basic benzoate and to determine the solubility of this compound. In this sense, the titration of each reactant (benzoic acid and zinc ion) and the titration of a solution containing both ions, with standardized sodium hydroxide, was carried out, at constant temperature (25 °C), in a thermostatized bath.

The solubility product constant (K_{sp}) of zinc hydroxide must be determined firstly in order to obtain K_{sp} of zinc basic benzoate. This was accomplished by titrating 5.00 mL of 0.1019 M zinc nitrate, acidified with 15.00 mL of 0.1065 M hydrochloric acid, in the absence of sodium benzoate and in the presence of 75.00 mL of 0.0188 M sodium benzoate. The final volume in the titration cell was kept constant in all cases. The titration of benzoic acid was also carried out to obtain the acid constant in the reaction medium employed in this research. The titrating solution was 0.1253 M sodium hydroxide. Reagent grade chemicals were used in all cases and the working temperature was maintained at 25 °C.

As it will be discussed later, titration curves showed the advantage of preparing zinc basic benzoate starting from 1.00 M ammonium benzoate and 0.33 M zinc nitrate. The zinc nitrate solution was dropped into the beaker containing 1 L of the benzoate solution, under continuous stirring. Once the addition of zinc nitrate was completed, the solution was stirred during 1 h. The precipitate was washed three times with 10^{-3} M ammonium benzoate to avoid hydrolysis of the precipitate; the supernatant liquid was then decanted. Finally, the precipitate was filtered off by means of a Büchner funnel and dried at 50 °C until constant weight.

The stoichiometry of the precipitate was determined weighing 0.2500 g of the precipitate and dissolving it in 180 mL of distilled water plus 20 mL H_2SO_4 1:1. The resulting solution was heated gently until complete dissolution was accomplished, cooled down to room temperature and placed in a 250 mL volumetric flask. An aliquot of 10 mL was treated with 5 mL of 1.000N $K_2Cr_2O_7$ plus 30 mL of concentrated H_2SO_4 and allowed to react 1 h at 50 °C in order to determine the benzoate content in the precipitate. Then 100 mL of distilled water was added to the beaker and the excess of potassium dichromate was back titrated with 0.5000N $FeSO_4$ in phosphoric medium, employing a potentiometric technique with platinum electrodes polarized with 5 μA. Iron was determined by indirect gravimetry, weighting 1.0000 g of zinc basic benzoate into a crucible. The sample was dried at 50 °C and then burned at 1100 °C.

Physicochemical properties of the pigment, relevant to paint technology, such as density (ASTM D 1475) and oil absorption (ASTM D 281), were measured, according to standardised procedures, in order to sketch a correct paint formulation.

The inhibitive properties of the anticorrosive pigment were evaluated by means of electrochemical techniques, employing SAE 1010 steel electrodes with low surface roughness (mean peak-to-valley height 1.40 μm). The corrosion potential was monitored as a function of time against a saturated calomel electrode (SCE) as reference. The supporting electrolyte was a pigment suspension in 0.025 M sodium perchlorat. Sodium perchlorate was chosen as supproting electrolyte in these preliminary studies to avoid the intense corrosion produced by sodium chloride which could make it impossible to observe the different processes which take place during corrosion. However, final essays on painted steel were carried out with both electrolytes.

The morphology of the protective layer formed on steel, at the open circuit potential, was studied by scanning electron microscopy (SEM) employing a PHILLIPS SEM 505 coupled with an EDAX OX PRIME 10 (energy dispersed form) to determine the surface elemental composition. Previous results showed the advantage of obtaining spectra of the reaction products from a mix of spectroscopical pure iron and zinc basic benzoate, molar ratio 1:1, which was wetted periodically with distilled water during a fortnight. The aim of this experience was to simulate the products which could be formed under a paint film in an accelerated test such as the salt spray chamber and identify those compounds which were responsible of the protection afforded by zinc basic benzoate. Products identification was carried out by spectroscopic techniques: UV–vis diffuse reflectance, FTIR and Mössbauer.

The reflectance spectra were recorded with a GBC CINTRA 40/UV–vis SPECTROMETER. Spectra were scanned in the 200–800 nm range at 50 nm/min. FTIR spectra were obtained with a Perkin-Elmer RX1 SPECTROMETER. The Mössbauer spectrometer was a conventional one of constant acceleration with a ^{57}Co(Rh) source of 20 mCi.

Steel corrosion rates, in pigment suspension in 0.5 M sodium perchlorate, at different exposure times, were obtained from polarisation resistance measurements. A SCE and a platinum grid were used as reference and counter electrodes, respectively. The swept amplitude was ±0.250 V from the open circuit potential and the scan rate 0.250 mV s^{-1}. Measurements were carried out with a Potentiostat/Galvanostat EG&G PAR Model 273 A plus SOFTCORR 352 software.

2.2. Paints composition, manufacture and application

Two different paints were formulated to carry out this research; one was the solvent-borne type (epoxy) and the other was an epoxy water-borne paint.

The resin employed to formulate the solvent-borne paint was a bisphenol epoxy-polyamide resin (1:1 ratio, by volume, v/v). The solvent employed was the mixture xylene/methyl isobutyl ketone/ butyl cellosolve (13/45/42%, by weight, w/w).

Table 1
Paint composition expressed as % by volume

Components	Solvent-borne paint (1)	Water-borne paint (2)
Zinc basic benzoate	13.3	3.5
Barium sulphate	12.2	2.2
Talc	12.2	2.1
Titanium dioxide	4.9	2.1
Zinc oxide	1.2	0.3
Mica	–	1.8
Resin/hardener (1/1 ratio)	28.4	–
Resin/hardener (1/1.2 ratio)	–	65.8
Additives	–	1.5
Solvents	27.8	20.7
Anti-corrosive pigment/total pigment (v/v)	30	30

It was decided to check the anticorrosive properties of the pigment employing a solvent borne paint because its behaviour has been well documented for many years. The pigment volume concentration/critical pigment volume concentration (PVC/CPVC) relationship was 0.8 as suggested elsewhere [41].

The anticorrosive pigment load was 30% (v/v) of the total pigment content; the same pigment content suggested when orthophosphates are employed as anticorrosive pigments [41,42]. Titanium dioxide, barium sulphate and talc were incorporated to complete the pigment formula. All pigments were dispersed for 24 h in the vehicle, employing a ball mill, to achieve an acceptable dispersion degree [43]. Paints formulations are shown in Table 1.

An epoxy resin, based on a mix of bisphenol A and bisphenol F, was chosen to formulate water-borne paints. The curing agent (hardener), which also acts as emulsifier, was a modified polyamidoamine with 50% of solids. The resin/hardener ratio was 100/120 (w/w). Neutral demineralized water was employed as solvent.

The anticorrosive pigment content was 30% of the total pigment content and titanium dioxide, barium sulphate, talc and mica were incorporated to complete the pigment formula. Mica was added to the formulation due to its barrier properties and ability to reduce the "flash rusting" degree [44]. The PVC values, 25%, were chosen in order to enhance the barrier properties of the coating.

The water-borne paint was prepared in a high-speed disperser. Preliminary tests showed the advantage of incorporating the pigment into the hardener, instead of mixing it with the resin. The relatively high viscosity of the hardener made it necessary to add, firstly, the water and then the pigments in accordance with their increasing oil absorption index; mica was added at last to avoid the break-up of laminar particles.

SAE 1010 steel panels (15.0 cm × 7.5 cm × 0.2 cm) were sandblasted to Sa 2 1/2 (SIS 05 59 00), degreased with toluene and then painted, by brushing, to reach a dry film thickness of 80 ± 5 μm. Painted panels were kept indoors for 14 days before testing.

2.3. Anticorrosive paint performance evaluation

2.3.1. Accelerated tests

For each type of paint, a set of three panels was placed in the salt spray chamber (ASTM B-117). Rusting (ASTM D-610) and blistering (ASTM D-714) degrees were evaluated after 4000 h of exposure.

Wet adhesion was also determined according to standard test (ASTM D 3359 method B). The coating on the steel panels was removed, after the exposition to the salt spray chamber, employing suitable solvents.

The morphology of the protective layer was observed by SEM, the surface elemental composition determined by EDAX and, finally, corrosion products were identified by UV–vis diffuse reflectance and FTIR Spectroscopy.

Another set of panels was placed in the humidity chamber, at 38 ± 1 °C (ASTM D 2247), for 2600 h. Rusting and blistering degrees were evaluated periodically, according to the above mentioned standard specifications.

2.3.2. EIS measurements

Impedance spectra of painted panels (frequency range 1.10^{-3} Hz $\leq f \leq 1.10^{5}$ Hz) were performed in the potentiostatic mode, at the corrosion potential. Measurements were done as a function of the exposure time to the electrolyte solutions (0.5 M $NaClO_4$ and 3% NaCl), using the 1255 Solartron FRA and the 1286 Solartron EI. The amplitude of the applied ac voltage was 0.010 V peak to peak. Two acrylic tubes were attached to each coated panel (working electrode) with an epoxy adhesive in order to perform the electrochemical measurements. The geometric area exposed to the electrolyte, each cell, was 15.9 cm^2. A large area Pt–Rh mesh of negligible impedance and saturated calomel (SCE) were employed as auxiliary and reference electrodes, respectively. The experimental impedance spectra were interpreted on the basis of equivalent electrical circuits using a suitable fitting procedure developed by Boukamp [45]. This electrochemical experiments were carried out at laboratory temperature (20 ± 2 °C), using a Faraday cage.

2.3.3. Equivalent circuits

The degradation of the paint system and the corrosion of the steel substrate, both take place through complex processes. The changes observed in the impedance spectra of the coated steel/electrolyte system, as a function of time, are originated in the dynamic nature of the conductivity through the paint film, the formation of corrosion products and disbondeding. Fortunately, appropriate equivalent circuit have been proposed (Fig. 1) in order to interpret and explain the time dependence of the resistive (R_i) and capacitive (C_i) parameters derived from fitting impedance data [46]. The fitting procedure is an accurate and less time consuming one, based in non-linear least squares algorithms [46–48].

Thus, equivalent circuits consisting of an arrangement of resistances (R_i) and capacitances (C_i), may be used to simulate the electrolytically conducting paths together with the faradaic process, occurring at the bottom of the paint film pores and under the film. So, R_1 is the electrolyte resistance between the

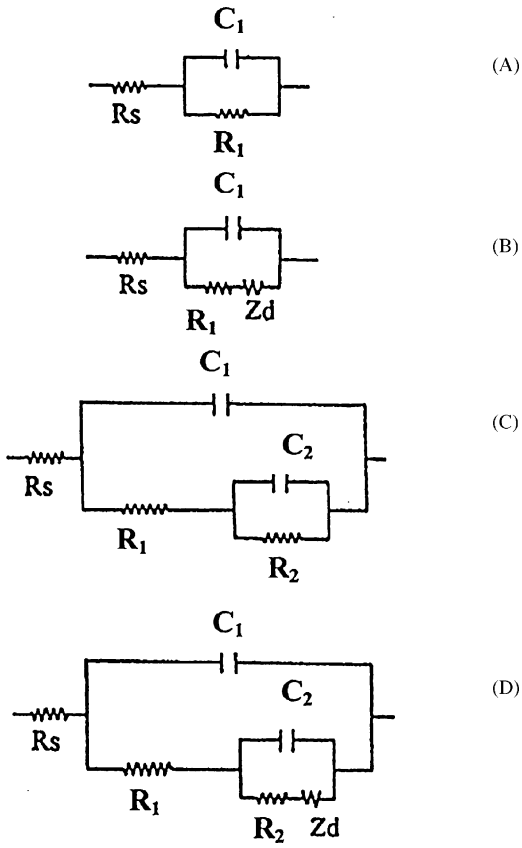

Fig. 1. The different equivalent circuits model the behaviour of organic coatings. (A) Intact coating; (B) a coating with a diffusion process across it; (C and D) a coating where the faradaic process associated with corrosion started.

reference (SCE) and working (coated steel) electrodes and represents the resistance to the ionic flux through different paths such as pores, low crosslinking areas, etc. These paths facilitate the penetration of the electrolyte solution towards the base metal. R_m is usually employed as a criterion of coating integrity together with C_1, the dielectric capacitance of the coating, which varies with the water uptake [49] and is determined by the intact part of the paint film. Once the permeating species (water, oxygen and ions) reach the electrochemically active areas of the substrate, at the bottom of the paint film pores, the corrosion process influences the observed impedance spectrum, and the associated parameters, i.e. the electrochemical double layer capacitance (C_2) and the charge transfer resistance (R_2), can be estimated from the impedance spectrum. R_2 and C_2 vary, respectively, inverse and directly with the attacked metallic area. As the exposure time goes on, a diffusion component Z_d became also measurable, which is related to the relaxation of a mass transport process, often linked with the oxygen reduction reaction [50].

Sometimes, when the bonding forces at the paint/substrate interface are weakened (e.g., by wet adhesion), a second faradaic process could be numerically separated and another time constant (R_3C_3) could be detected [49]. This process takes place under intact parts of the coating film and is originated by the lateral diffusion of the electrolyte.

3. Results and discussion

3.1. The precipitate–solution equilibrium between zinc cation and benzoate anion

The analysis of the precipitate obtained when benzoate anion reacted with zinc cation revealed that there was one mole of benzoate per each mole of zinc cation; so it was concluded that the precipitate formula was ZnBOH.

K_{sp} of zinc hydroxide could be calculated as follow. Let V_1 be the base volume employed to titrate hydrochloric acid in the sample containing only zinc cation (Fig. 2), according to the equation:

$$H_3O^+ + OH^- \rightarrow 2H_2O$$

and V_2 the volume of base solution required to precipitate zinc cation:

$$Zn^{+2} + 2OH^- \rightarrow Zn(OH)_2$$

The expression for K_{sp} of zinc hydroxide may be written as follows:

$$K_{sp}[Zn(OH)_2] = [Zn^{+2}][OH^-]^2$$

and calculated by the equation:

$$K_{sp}[Zn(OH)_2] = \left[\frac{1/2(V_2 - V_a)M}{V_i + V_a}\right]\frac{K_W^2}{[H_3O^+]^2} \quad (1)$$

where V_a is a base volume corresponding, normally, to the middle point of the plateau defined when zinc hydroxide precipitated. From experimental data in Fig. 2, $V_2 = 27.50$ mL and the K_{sp} for zinc hydroxide, calculated from the previous equation, resulted equal to 1.52×10^{-17}, being the value reported in the literature 7.50×10^{-18} [51].

The precipitation curve of zinc benzoate was ill-defined and two different zones could be distinguished. One of them was comprised between pH 3.00 and 5.00, approximately; and the other between two inflection points located at 17.96 and

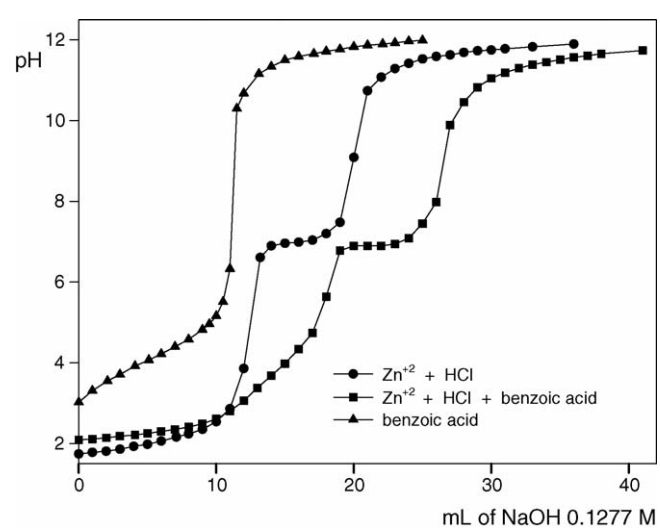

Fig. 2. Titration curves of different systems as a function of the volume of 0.1253 M sodium hydroxide.

26.52 mL, respectively. The first zone corresponds to the precipitation of a zinc compound but no plateau was defined as it occurred in the second zone. This fact may be attributed to a slow precipitation or to the occurrence of more than one precipitation reaction. The pH of the plateau in the second zone was that of the precipitation of zinc hydroxide. So, it was concluded that zinc hydroxide is precipitating in this second zone and that hydroxyl ion was replacing the ligand of the compound formed in the first zone. For this reason, K_{sp} of zinc basic benzoate was determined from 0.1019 M sodium benzoate solution to which the milli-moles of zinc cation, necessary to precipitate half of the amount of sodium benzoate, were added. Then, the final pH of the system (5.63) was measured employing a glass electrode.

The acid constant of benzoic acid was obtained from the titration curve of benzoic acid, following the procedure described in the literature [51,52]. The calculated value was 8.04×10^{-5}; very close to that reported by Wilson and Wilson [51] (6.30×10^{-5}) in the literature.

The equations for the dissociation of zinc basic benzote and the hydrolysis of benzoate anion and the cation are as follows; the constants associated with each equilibrium are written and calculated below.

$$\mathrm{ZnBOH} \rightarrow \mathrm{Zn}^{+2} + \mathrm{OH}^- + \mathrm{B}^-$$

$$K_{sp}[\mathrm{ZnBOH}] = [\mathrm{B}^-][\mathrm{OH}^-][\mathrm{Zn}^{2+}]$$

$$\mathrm{B}^- + \mathrm{H_2O} \Leftrightarrow \mathrm{HB} + \mathrm{OH}^-$$

$$K^{h}_{B^-} = \frac{[\mathrm{HB}][\mathrm{OH}^-]}{[\mathrm{B}^-]} = \frac{K_W}{K_a} \Rightarrow K^{h}_{B^-} = 1.24 \times 10^{-10}$$

$$\mathrm{Zn}^{2+} + 4\mathrm{H_2O} \Leftrightarrow \mathrm{Zn(OH)_2} + 2\mathrm{H_3O}^+$$

$$K^{h}_{Zn} = \frac{[\mathrm{H_3O}^+]^2}{[\mathrm{Zn}^{2+}]} = \frac{[\mathrm{H_3O}^+]^2[\mathrm{OH}^-]^2}{K_{\mathrm{spZn(OH)_2}}} = \frac{K_W^2}{K_{\mathrm{spZn(OH)_2}}} \Rightarrow K^{h}_{Zn} = 6.58 \times 10^{-12}$$

The hydrolysis constant of the cation do not differ significantly from that of the anion. Moreover, the analysis of the precipitate in the first zone of the titration curve revealed the co-precipitation of zinc hydroxide. As a consequence, K_{sp} of basic zinc benzoate was calculated taking into account that zinc basic benzoate was in equilibrium with zinc hydroxide; so, the concentration of the cation could be replaced from the expression of $K_{sp}[\mathrm{Zn(OH)_2}]$, thus obtaining:

$$K_{sp}[\mathrm{ZnOHB}] = [\mathrm{B}^-]^3 \frac{K_{sp}[\mathrm{Zn(OH)_2}]}{[\mathrm{OH}^-]}$$

The value of $K_{sp}[\mathrm{ZnOHB}] = 3.52 \times 10^{-10}$ was easily obtained and the solubility of the compound calculated. The theoretical solubility value was found to be 7.06×10^{-4} M (144 ppm) while the experimental value, obtained by indirect gravimetry, was 160 ppm.

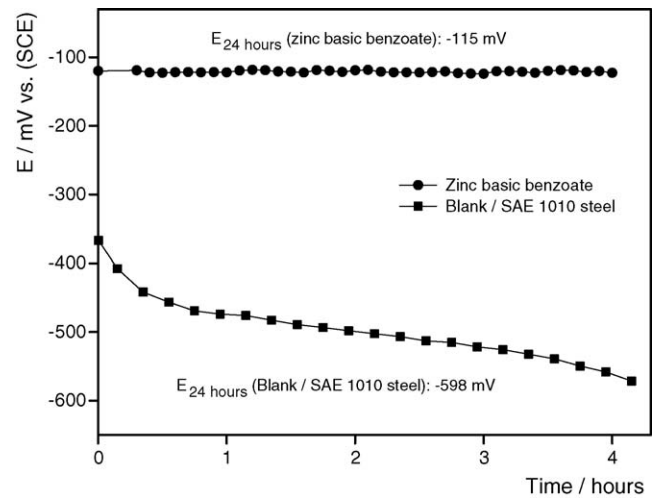

Fig. 3. Corrosion potential of SAE 1010 steel in zinc basic benzoate in 0.5 M $NaClO_4$ suspensions.

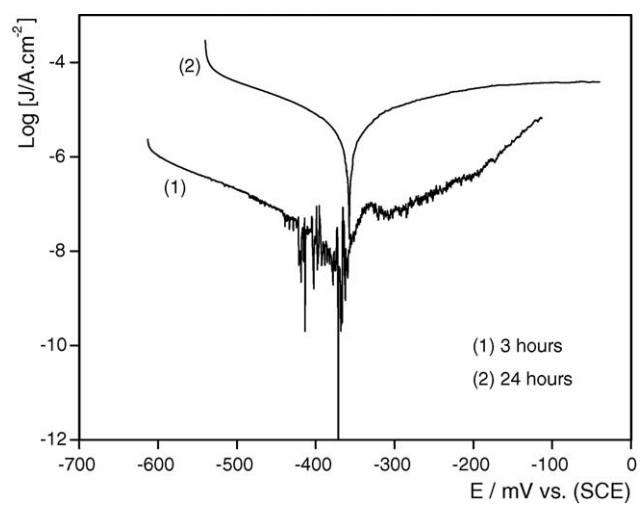

Fig. 4. Tafel plots of the SAE 1010 steel electrode in zinc basic benzoate suspensions in 0.5 M $NaClO_4$, at different exposure times.

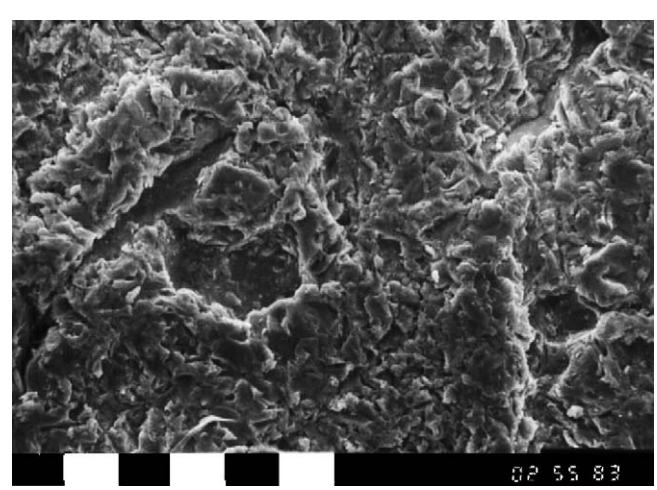

Fig. 5. SEM micrograph of the steel surface after being in contact 24 h with zinc basic benzoate suspension in 0.025 M$NaClO_4$ (magnification 1000×).

3.2. Electrochemical assessment of the anticorrosive properties of basic zinc benzoate

The corrosion potential versus time curve revealed that zinc basic benzoate displaced the electrode potential towards ∼−100 mV versus SCE, being this value much more positive than that of SAE 1010 steel in the supporting electrolyte (−650 to −750 mV versus SCE) (Fig. 3).

Steel dissolution in zinc benzoate suspension, after 3 h of exposure, was rather polarized and the curve exhibited an ill-defined passivation peak at ∼−350 mV (Fig. 4). The cathodic current in the plateau was too low, 65 nA cm^{-2}, which would

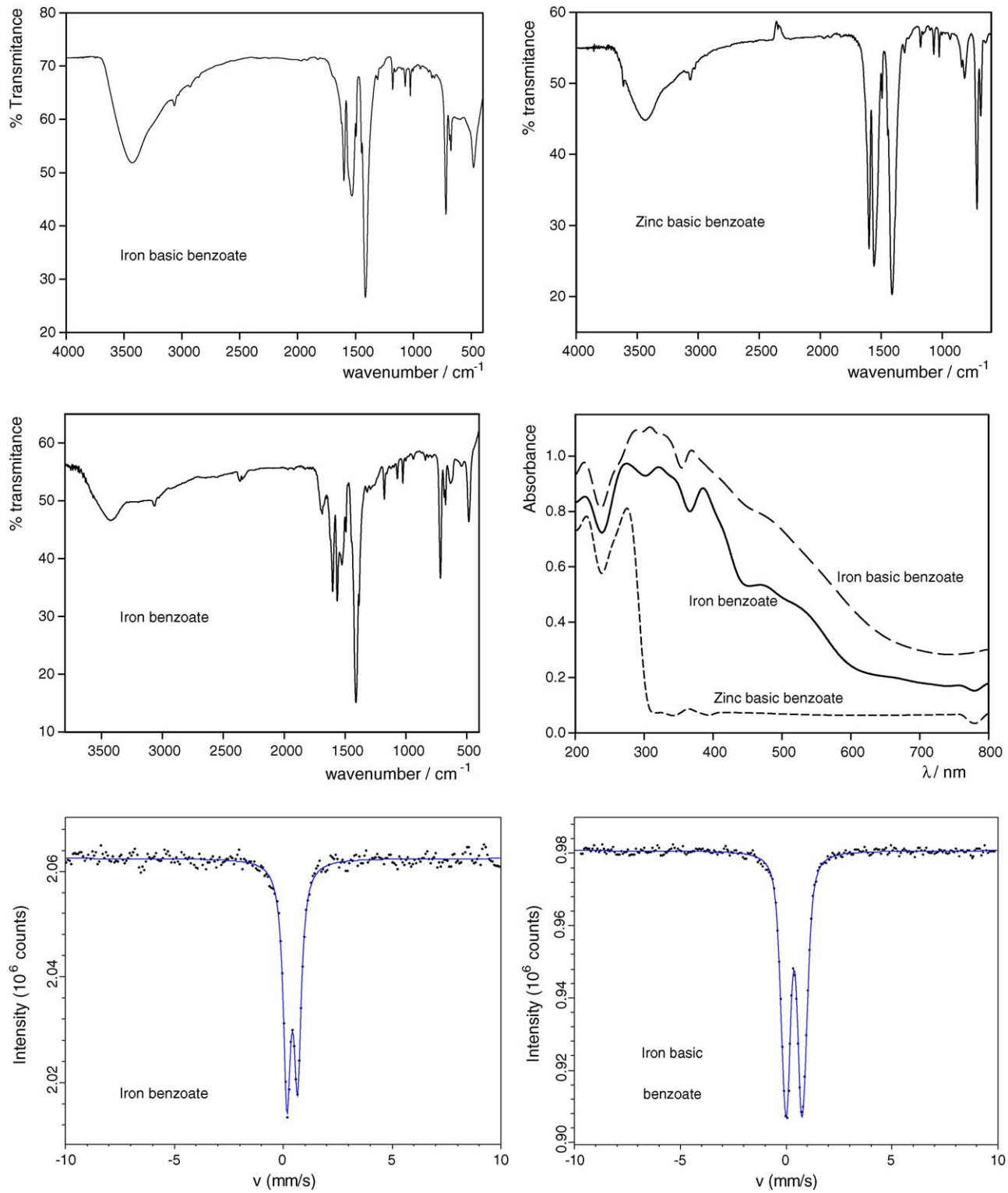

Fig. 6. UV–vis diffuse reflectance, FTIR and Mössbauer spectra of zinc basic benzoate and iron benzoates.

point out that cathodic reactions were inhibited if one takes into account that the cathodic current density measured with a platinum electrode in the supporting electrolyte was 220 μA cm^{-2}. After 24 h of exposure the anodic reaction was much more polarized, that is to say that the slope of the I versus E curve was lower. The cathodic current increased to 20 μA cm^{-2} but it was still lower than the oxygen current on platinum. Corrosion rate, obtained from Tafel plots, was 58.6 nA cm^{-2} after 3 h of exposure and 3.50 μA cm^{-2} after 1 day has elapsed. These facts, together with the displacement of E_{corr} to ~-100 mV, led to the conclusion that zinc basic benzoate was able to inhibit corrosion.

The protective layer, formed at the corrosion potential, was an uniform oxide film, constituted basically by iron oxides and oxyhydroxides (Fig. 5). As a general rule, no zinc was detected on the protective layer.

3.3. The nature of corrosion products formed during the reaction of iron and basic zinc benzoate

The nature of the corrosion products formed as a consequence of the heterogeneous reaction between iron and zinc basic benzoate was investigated by means of spectroscopic techniques, as it was said previously. UV–vis diffuse reflectance, FTIR and Mössbauer spectra of zinc benzoate, iron benzoate and iron basic benzoate were obtained (Fig. 6) because iron benzoates could be formed during the corrosion reaction and unreacted zinc basic benzoate could be found in the mixtures. The procedure employed to obtain iron benzoate was described elsewhere [53].

UV–vis spectra were deconvoluted by adjusting the spectral curve with multiple Gaussian peaks with a routine provided with the software MICROCAL ORIGIN 6.0. The fitting accuracy was assessed with the parameter χ^2 which was comprised between 1–4 × 10^{-5}. Band assignment for iron oxides and oxyhydroxides was carried out employing the wavelength chart compiled by Larramona and Gutiérrez [54]. Mössbauer spectra analysis was made by means of the Recoil program, employing Lorentzian lines.

The UV–vis spectrum of ferric benzoate exhibited several important bands at 218–224 (characteristic of benzoates), 274, 322 and 398 nm, respectively. The most important bands of iron basic benzoate are located at 215, 287 and 371 nm. The UV–vis spectrum of zinc basic benzoate only possesses two important bands at 214 and 273 nm. The FTIR spectrum of ferric benzoate exhibited, in the frequency group region, the following bands: 1412, 1493, 1525, 1564, 1601, 1687, 3064 and 3423 cm^{-1}. Ferric basic benzoate has a similar FTIR spectrum but it does not posses the bands located at 1493, 1566 and 1674 cm^{-1}; being the band at 1674 cm^{-1} the most intense band which could be used to differentiate both types of iron benzoates. The FTIR spectrum of zinc basic benzoate was quite similar to that of ferric benzoate but the bands at 1525 and 1687 cm^{-1} did not appear in the corresponding spectrum. The Mössbauer spectrum corresponding either iron benzoate or to iron basic benzoate, both had central asymmetric doublet originated by a high spin ferric compound. The most characteristic Mössbauer parameters, isomer shift and average quadrupole splitting are different for both compounds. Isomer shift was 0.42 for iron benzoate and 0.38 for basic iron benzoate while the quadrupole splitting was 0.49 for the former compound and 0.81 for the last one (Fig. 6).

The deconvolution of UV–vis spectrum revealed that neither iron oxides nor iron oxyhidroxides were formed during the corrosion reaction. The low intensity band at 374 nm could indicate

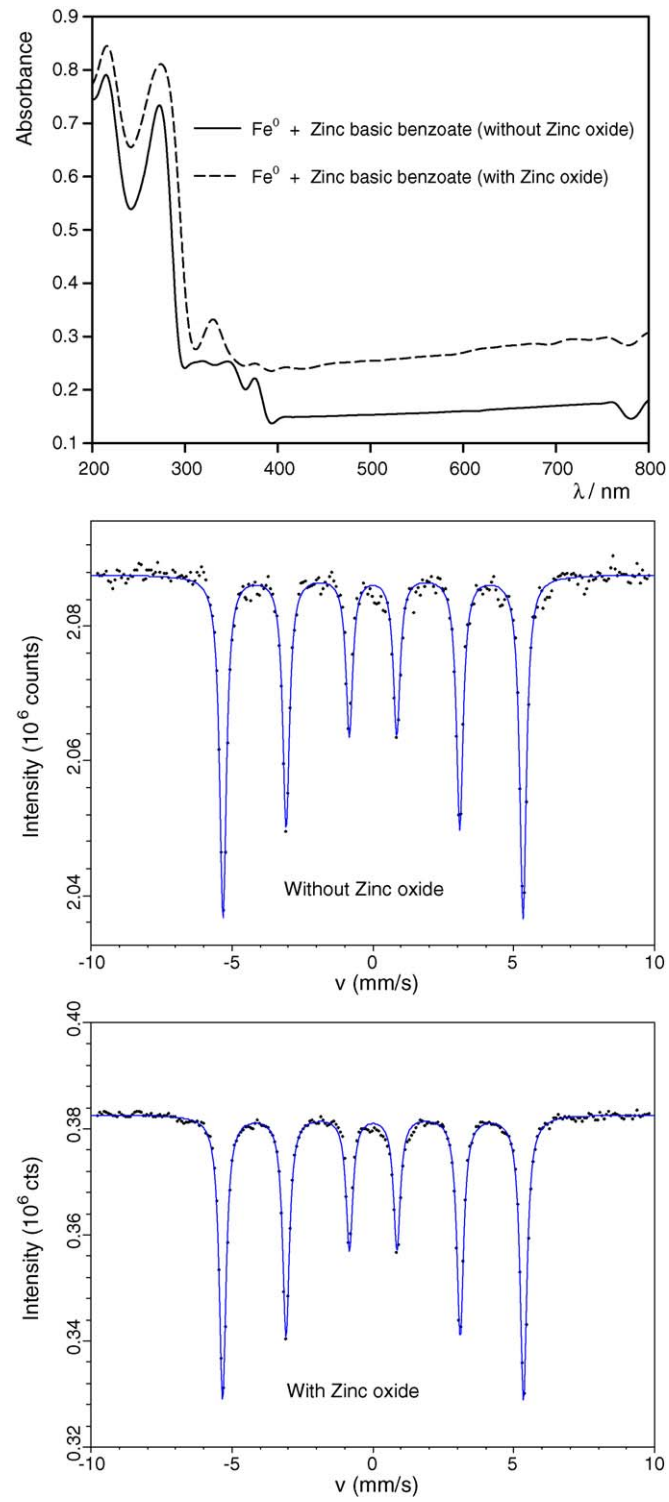

Fig. 7. UV–vis diffuse reflectance, FTIR and Mössbauer spectra of the iron/zinc basic benzoate mix.

Table 2
Rusting[a] (ASTM D 610) and blistering[b] (ASTM D 714) degrees of the painted panels exposed to the salt spray chamber (ASTM B 117)

Paints		Time (h)									
		310	770	980	1150	1400	1580	1800	2500	3600	4000
1	R	10	9	9	8	7	6	–	–	–	–
	B	10	8F	6F	6F	4M	4MD	–	–	–	–
2	R	10	9	9	9	9	9	8	8	7	6
	B	10	10	10	10	10	10	10	8F	8F	8F

R[a]: rusting degree (ASTM D 610)

Rust grade	10	9	8	7	6	5	4	3	2	1
Rusted area (%)	No rusted	0.03	0.1	0.3	1	3	10	16	33	50

B[b]: blistering degree (ASTM D 714)

Frequency	Dense, D	Medium dense, MD	Medium, M	Few, F
Size	10	8	6, 4	2
Comments	No blistering	Smaller size blister easily seen by unaided eye	Progressively larger sizes	

that small amounts of iron basic benzoate were formed. The presence of unreacted zinc benozate was confirmed by the characteristic bands in the IR and UV–vis region. The Mössbauer spectrum only showed the iron sextet, thus indicating the absence of appreciable reaction between iron and zinc basic benzoate and confirming the inhibitive properties of zinc basic benzoate. The central doublet corresponding to an iron benzoate could not be detected in the spectrum (Fig. 7).

The foregoing discussion pointed out that corrosion products could be easily identified by UV–vis spectroscopy; for this reason the qualitative analysis of the protective layer, under the paint film, described later, was carried out only by this technique.

3.4. The performance of anticorrosive paints through accelerated tests

The best anticorrosive behaviour in the salt spray test was achieved with the water-borne paint (paint 2) whose qualification was seven after 3600 h of exposure (Table 2). The solvent-borne epoxy (paint 1) had a poorer anticorrosive behaviour because the same qualification was attained after 1400 h of exposure. In spite of the very important differences observed in this test, it may be pointed out that both types of paints behaved satisfactorily, specially the water-borne paint. The blistering process was also much less severe in the case of the water-borne epoxy because the first blisters were observed around 2500 h of exposure and they were of small size and low surface density.

Although wet adhesion was higher for the water-borne paint than for the solvent-borne epoxy, the adhesion of the former begun to decrease after 640 h in the salt spray chamber (Table 3). However, the substrate remained protected beyond 3600 h due to the inhibitive action of the pigment.

Both paints had a similar corrosion resistance in the humidity chamber (Table 4) which was lower than in the salt spray test. The qualification seven was obtained, in both cases, after 2100 h of exposition. Both paints also developed a similar blistering process although the solvent-borne epoxy paint was the latest in exhibiting blistering which was detected after 1150 h of exposure. After 2100 h rather high sized blisters (6) have grown on the surface with a relatively high surface density (MD).

The anticorrosive behaviour of this pigment may be compared with its predecessor, zinc phosphate. The comparison between zinc basic benzoate and zinc phosphate is rather complicated because there are several products in the market, each one of different quality. Epoxy paints formulated with zinc phosphate of good quality begun to fail, as an average, after 1700 h of exposure in the salt spray test as similar paints formulated with basic zinc basic benzoate did. It was reported that water-borne paints pigmented with zinc phosphate behaved satisfactorily during 2400 h of exposure in the salt spray chamber (qualifi-

Table 3
Wet adhesion [a]test (ASTM D 3359) of painted panels as a function of the exposure time to the salt spray chamber (ASTM B 117)

Paint	Time (h)								
	0	48	120	350	640	956	1300	1800	2400
1	5B	4B	3B	3B	2B	1B	–	–	–
2	5B	5B	5B	5B	4B	4B	4B	3B	3B

[a]Tape-test method B (ASTM D 3359/97)

Classification	5B	4B	3B	2B	1B	0B
Removed area (%)	0	<5	5–15	15–35	35–65	>65

Table 4
Rusting (ASTM D 610) and blistering (ASTM D 714) degrees of the painted panels exposed to the humidity chamber (ASTM B 2247)

Paints		Time (h)								
		480	770	980	1150	1400	1580	1800	2100	2600
1	R	10	10	9	8	8	8	8	7	6
	B	10	10	10	6M	6M	6MD	6MD	6MD	4D
2	R	10	10	9	9	8	8	7	7	6
	B	10	6F	6M	6M	6M	6M	6MD	6MD	6MD

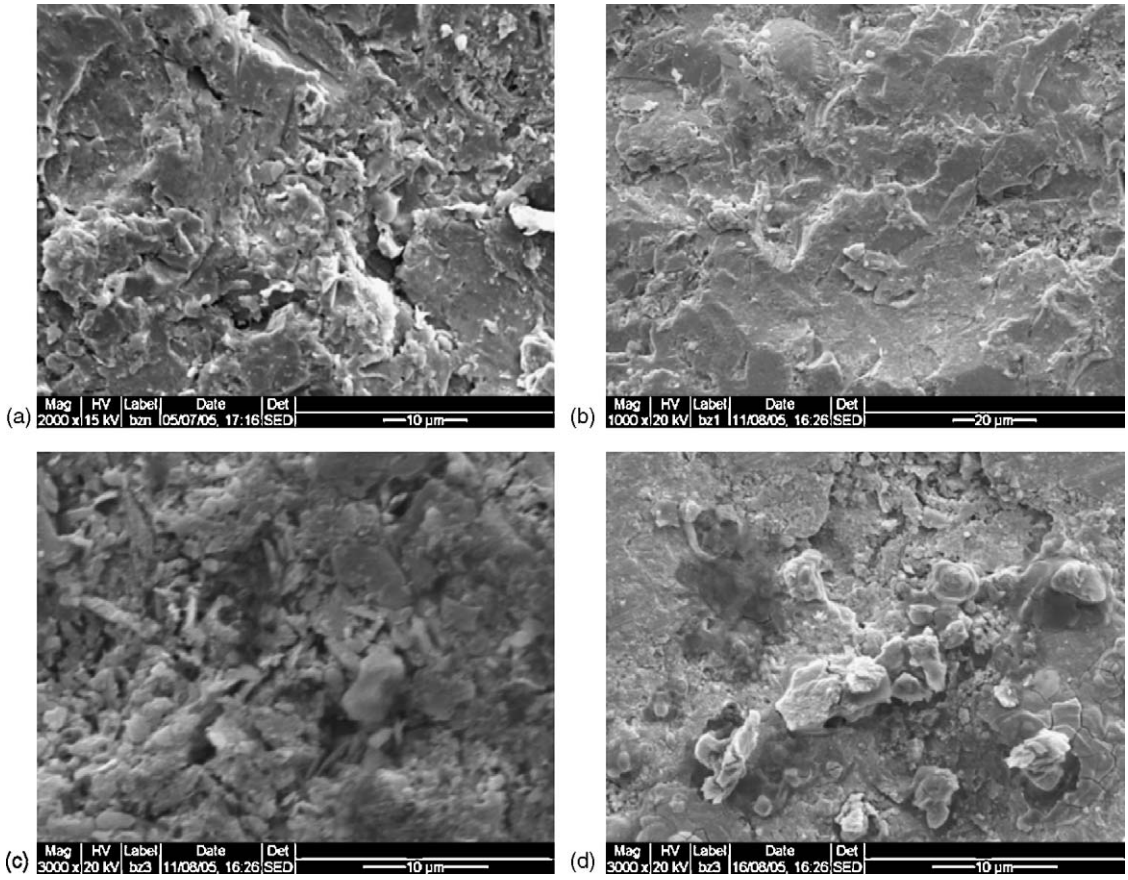

Fig. 8. SEM micrograph of the steel surface after removing the different coatings on panels exposed to the salt spray chamber (ASTM B 117). Magnification: (a) 2000×, (b) 1000×, (c and d) 3000×.

cation 10) while paints formulated with basic zinc phosphate underwent 3600 h of exposure with an acceptable anticorrosive behaviour [55]. This led to the conclusion that basic zinc benzoate is able to replace zinc phosphate with equal or even better performance, especially in water-borne paints.

The epoxy paint formulated with zinc basic benzoate was more resistance to blistering because it appeared at 1150 h while the process for epoxy paints formulated with zinc phosphate begun, in all cases, after 750 h of exposure. Water-borne paints formulated either with zinc basic benzoate or with zinc phosphate did not show much resistance to blistering due to the nature of the binder which tended to re-emulsification [55].

Steel panel surface morphology was studied by SEM, after removing the organic coating with suitable solvents. Xylene was employed for softening the paint film which was finally removed with THF and/or 1-methyl-2-pyrrolidon. A more or less uniform film constituted basically by non expansive iron oxides was formed under both epoxy coatings (Fig. 8a and b). The average elemental composition of the film was C: 10.3%, O: 6.1%, Zn: 2.3%, Al: 1.4%, Si: 6.1% and Fe: 73.8%. Laminar talc particles were also observed on the oxide film. There also existed certain zones, presumably with higher galvanic activity, where the oxide layer was discontinued and small particles of iron oxide formed together with crystalline iron oxides (Fig. 8c). In certain areas, film rupture could be appreciated together with spherical formations (Fig. 8d) whose average composition was as follows: C: 2.1%, O: 21.6%, Zn: 0.4%, Al: 1.1%, Si: 0.7%, Cl: 7.6%, Fe: 66.5%. These formations are thought to be the nucleus which facilitates the growth of expansive iron oxides.

The compounds which constitute the protective layer were identified by UV–vis diffuse reflectance spectroscopy (Fig. 9). The protective layer formed below the solvent-borne epoxy coat-

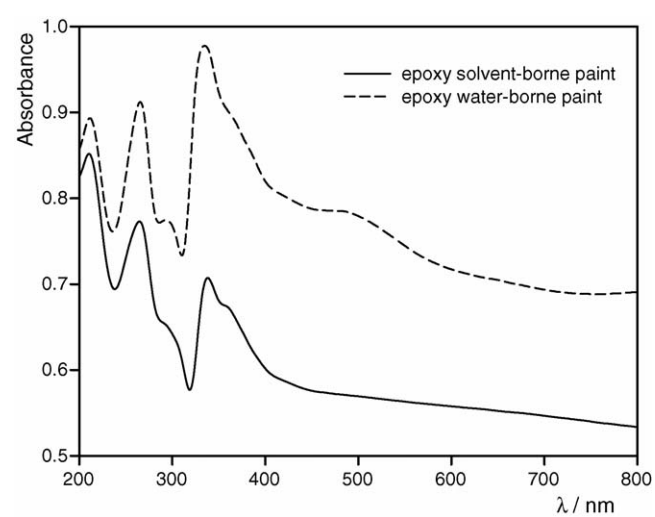

Fig. 9. UV–vis diffuse reflectance spectra of steel surface exposed to the salt spray, after paint removal by suitable solvents.

ing contained α-FeOOH (goethite) but γ-FeOOH (lepidocrosite) was not found in it due to the absence of one of its characteristic bands at 700 nm. The spectrum of α-FeOOH could exhibit a variable width band between 380 and 432 nm, depending on the particle size, and another band at 646 nm; both were encountered during the deconvolution process [54]. The presence of α-Fe_2O_3 was evidenced by the absorption bands at 533–566 (variable width), 360 and 500 nm [54]. It is not strange the presence of both compounds because α-FeOOH is the hydrated form of α-Fe_2O_3. The characteristic bands of iron benzoate and iron basic benzoate were also detected although they overlapped with the bands corresponding to the oxides and oxyhidroxides.

The deconvolution of the spectrum of the steel surface covered with the paint formulated with the water-borne resin also showed the presence of different iron oxides and oxyhydroxides. As in the case of the solvent-borne paint, deleterious lepidocrosite (γ-FeOOH) was not detected [54]. The existence of α-Fe_2O_3 was evidenced by the reported bands at 280, 360 and 500 nm [49]. It was suspected that γ-Fe_2O_3 could be formed due to the presence of a band at ∼600 nm. The bands of iron benzoates were also detected. The presence of benzoates would explain the carbon content found by EDAX analysis of the protective layer. The presence of oxides and hydroxides in the protective layer, not found among the corrosion products in the mix iron/zinc iron benzoate, was attributed to the long exposure time in the salt spray test.

3.5. EIS measurements

The relative performance of painted steel samples, submerged in 0.5 M NaCl solution, was evaluated by measuring the corrosion potential (Fig. 10) and by analysing the variation of R_i and C_i with the exposure time (Fig. 11).

The epoxy solvent-borne paint showed an unusual behaviour in 3% NaCl, in the sense that the corrosion potential diminished within 3 weeks of immersion, below −300 mV. It was thought that there must be certain incompatibility between the pigment and the binder which is highlighted by the aggressiveness of the supporting electrolyte. The same paint showed a very different behaviour in 0.5 M $NaClO_4$ and the steel corrosion potential remained displaced towards more positive values for a longer period of time exhibiting, at the same time, a slight tendency to repassivation beyond 60 days of immersion.

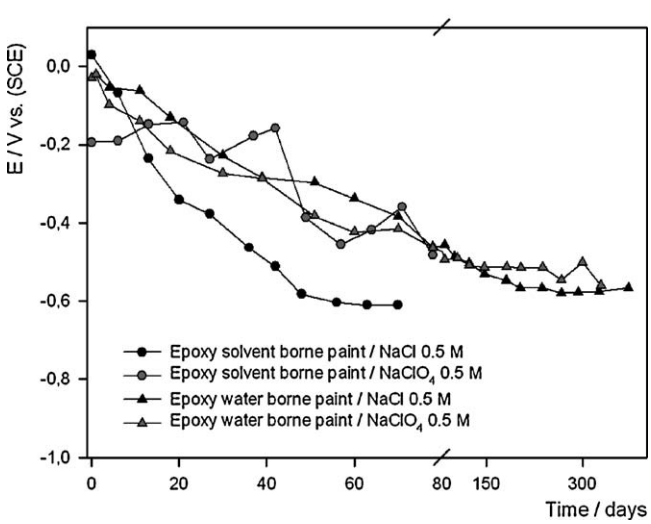

Fig. 10. Corrosion potential of coated steel in 0.5 M NaClO4 and 3% NaCl.

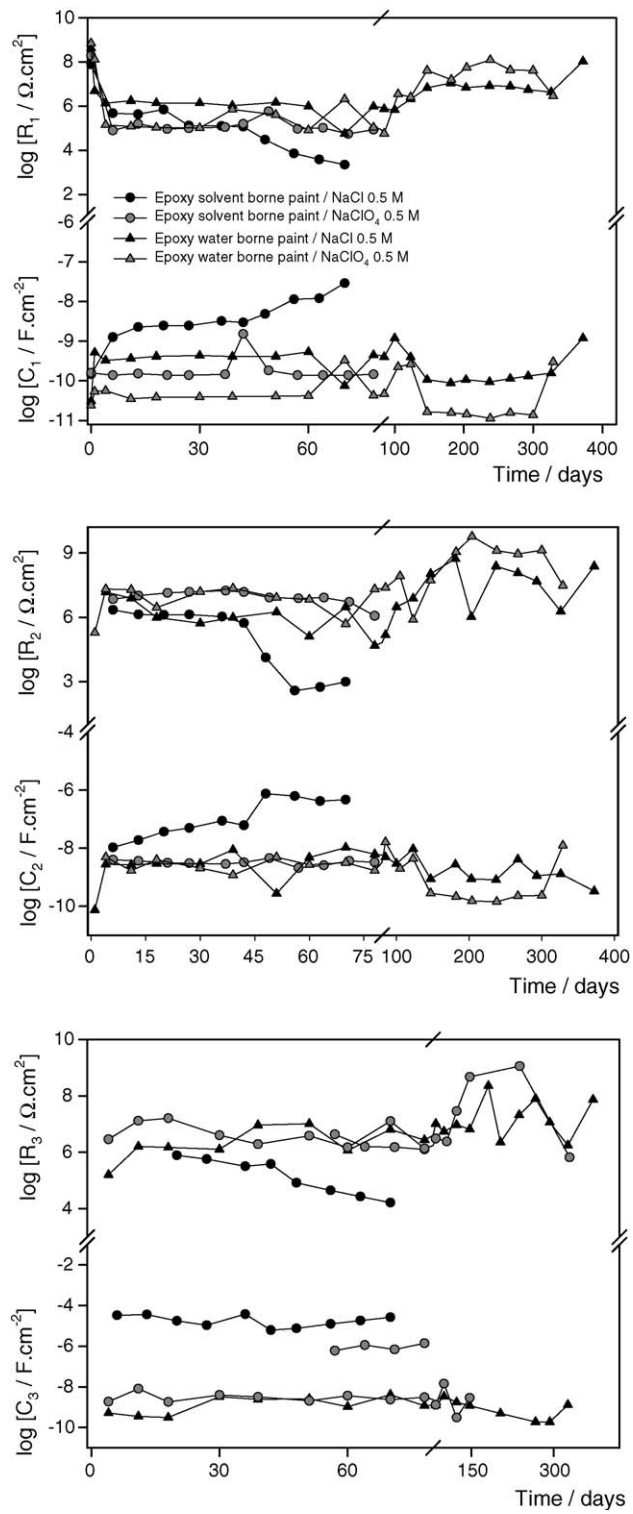

Fig. 11. Fitting parameters, R_i and C_i, for the different coatings, as a function of the immersion time in 0.5 M $NaClO_4$ and 3% NaCl.

The water-borne epoxy paint underwent an extended immersion period, approximately 300 days of immersion, without showing signs of corrosion in both electrolytes.

Both paints developed a high initial barrier effect ($R_1 > 10^8\ \Omega\,cm^{-2}$) which was rapidly lost before 10 days of immersion; however, values fluctuated between 10^5 and $10^6\ \Omega\,cm^{-2}$, pointing out that a residual barrier effect is still present [56–58]. The exception to the rule was the solvent-borne epoxy paint whose ionic resistance decreased from 40 days of immersion. In change, the water-borne coating showed a sudden increase in the barrier properties after 100 days of immersion, matching values higher than $10^8\ \Omega\,cm^{-2}$. This property, together with the high values measured for the parameter R_2, suggested that this pigment very adequate to formulate water-borne coatings with improved performance. C_1 values are in close relationship with R_1 values, that is to say the solvent borne paint exhibited higher values than the water-borne one, in both electrolytes, due to the deterioration of the film after water permeation.

The parameters associated with the faradaic reaction (R_2, C_2) are similar in both electrolytes but the solvent-borne epoxy paint degraded previously in NaCl 3%; however, its anticorrosive behaviour was still satisfactory until 45 days of immersion. R_2 maintained higher than $10^6\ \Omega\,cm^{-2}$ during 100 days for the solvent-borne paint in 0.5 M $NaClO_4$ and for more than 1 year for the water-borne coating in both electrolyte. In the case of this last coating, the charge transfer resistance increased over $10^9\ \Omega\,cm^{-2}$ in 0.5 M $NaClO_4$ which is, a very high value for an anticorrosive coating. This features, together with the prolonged life of the water-borne coating in immersion, point out the fact that zinc basic benzoate is a very useful pigment to formulate ecological anticorrosive coatings. In accordance with above discussion, C_2 values indicate that the active area is small in the water-borne paint and reached typical values of uncoated steel in the case of the solvent-borne paint in NaCl 3%.

The appearance of a third constant time (R_3, C_3) pointed out the existence of an under film corrosion process. The initiation of this process depended on the binder type and on the aggressiveness of the electrolyte. The water-borne paint was more prone to this type of corrosion due to the tendency of the binder to re-emulsify but the high value of R_3 showed that the substrate was being protected by the pigment.

4. Conclusions

1. Zinc basic benzoate could be adequately precipitated from sodium benzoate solution. The pigment solubility was adequate to formulate anticorrosive paints.
2. The electrochemical tests performed employing pigment suspensions confirmed the anticorrosive properties of the inhibitor.
3. The protective layer formed on steel could be formed by iron oxides or oxyhydroxides, predominantly α-forms, as well as iron benzoates.
4. UV–vis diffuse reflectance spectroscopy proved to be a very useful tool to investigate the metallic surface once the coating has been removed.
5. Accelerated tests showed that zinc basic benzoate also performed satisfactorily in paints. The best results were obtained with the water-borne paint which underwent 3600 h of exposure in the salt spray chamber.
6. Electrochemical tests showed that the pigment generated very high charge transfer resistance values which were responsible of the protection afforded by the paints. The barrier properties were of much less importance.

Acknowledgements

The authors are grateful to: CONICET (Consejo Nacional de Investigaciones Científicas y Técnicas), CICPBA (Comisión de Investigaciones Científicas) and UNLP (Universidad Nacional de La Plata) for their sponsorship to do this research.

References

[1] D. Eurof Davies, Q.J.M. Slaiman, Mechanism of the corrosion inhibition of Fe by sodium benzoate-I. The influence of concentration and pH in air-saturated solutions of sodium benzoate, Corros. Sci. 11 (1971) 671.
[2] Q.J.M. Slaiman, D. Eurof Davies, Mechanism of the corrosion inhibition of Fe by sodium benzoate-II. The inhibitive properties of sodium benzoate in de-aerated and air-saturated solution, Corros. Sci. 11 (1971) 683.
[3] D. Eurof Davies, Q.J.M. Slaiman, Mechanism of the corrosion inhibition of iron by sodium benzoate-III. The role of oxygen, Corros. Sci. 13 (1973) 891.
[4] V.S. Muralidharan, R. Sethuraman, S. Krishnamoorthy, Benzoic acid as corrosion inhibitors for pure iron in sulphuric acid, Bull. Electrochem. 4 (1988) 705.
[5] D.S. Azambuja, L.R. Holzle, I.L. Muller, C.M.S. Piatnicki, Electrochemical behaviour of iron in neutral solutions of acetate and benzoate anions, Corros. Sci. 41 (1999) 2083.
[6] M. Yamaguchi, H. Nishihara, K. Aramaki, The inhibition of passive film breakdown on iron in a borate buffer solution containing chloride ions by anion inhibitors, Corros. Sci. 36 (1994) 241.
[7] M. Ergun, A.Y. Turan, Pitting potential and protection potential of carbon steel for chloride ion and the effectiveness of different inhibiting anions, Corros. Sci. 32 (1991) 1137.
[8] V. Otieno-Alego, G.A. Hope, H.J. Flitt, G.A. Cash, D.P. Schweinsberg, The effect of potential scan on the parameters used to synthesize anodic polarization curves, Corros. Sci. 33 (1992) 1719.
[9] R. Kahraman, A.A. Al-Mathami, H. Saricimen, N. Abbas, S.U. Arman, A study of corrosion control of carbon steel using inhibitors in a simulated environment, Anticorros. Methods Mater. 49 (2002) 346.
[10] P. Argawal, D. Landolt, Effect of anions on the efficiency or aromatic carboxylic acid corrosion inhibitors in near neutral media: experimental investigation and theoretical modeling, Corros. Sci. 4–5 (1998) 673.
[11] R. Kahraman, Inhibition of atmospheric corrosion of mild steel by sodium benzoate treatment, J. Mater. Eng. Perform. 11 (2002) 46.
[12] K. Takahashi, J.A. Bardwell, B. Mac Dougall, M.J. Graham, Mechanism of anodic dissolution and passivation of iron-II. Comparison of the behavior in neutral benzoate and acetate buffer solutions, Electrochim. Acta 37 (1992) 489.
[13] J.R. Culleré, M. Lluveras, Mecanismo de la acción inhibidora del benzoato sódico, Revista Iberoamericana de Corrosión y Protección (1983) 225.
[14] G. Bondietti, J. Sinniger, W. Stumm, The reactivity of FE(III) (hydr)oxides: effects of ligands in inhibiting the dissolution, Colloids Surf., A: Physicochem. Eng. Aspect 79 (1993) 157.
[15] R. Kahraman, H. Saricimen, M. Al-Zahrani, S. Al-Dulaijan, Effect of inhibitor treatment on corrosion of steel in a salt solution, J. Mater. Eng. perform. 12 (2003) 524.

[16] O. Lahodny-Šarc, F. Kapor, Corrosion inhibition of carbon steel by blends of gluconate/benzoate at temperatures up to 60°C, Mater. Sci. Forum 289–292 (1998) 1205.
[17] G. Blustein, J. Rodríguez, C.F. Zinola, R. Romagnoli, Adsorption and inhibition of steel corrosion by calcium benzoate in nitrate solutions, Corros. Sci. 47 (2005) 369.
[18] P.N.S. Yadav, A.K. Singh, R. Wadhwani, Role of hydroxyl group in the inhibitive action of benzoic acid toward corrosion of aluminium in nitric acid, Corrosion (NACE) 55 (1999) 937.
[19] A. Raspini, Influence of sodium salts of organic acid as additives on localized corrosion of aluminium and its alloys, Corrosion (NACE) 49 (1993) 821.
[20] A.K. Mohamed, S.A. Abd El-Maksoud, A.S. Fonda, p-Substituted benzoic acid derivatives as corrosion inhibitors for aluminium in H_3PO_4, Portugaliae Electrochim. Acta 15 (1997) 27.
[21] S. Zor, The effects of benzoic acid in chloride solutions on the corrosion of iron and aluminium, Turk. J. Chem. 26 (2002) 403.
[22] W.J. Rudd, J.C. Scully, The function of the repassivation process in the inhibition of pitting corrosion on aluminium, Corros. Sci. 20 (1980) 611.
[23] K. Aramaki, Effects of organic inhibitors on corrosion of zinc in aerated 0.5 M NaCl solution, Corros. Sci. 43 (2001) 1985.
[24] S.M. Abd El Haleem, A.A. Abdel Fattah, The role of some organic anions in promoting or inhibiting the corrosion of zinc, Surf. Coat. Technol. 29 (1986) 41.
[25] S.N. Mostafa, M.Y. Mourand, S.A. Seliman, Electrochemical studies on the corrosion of cooper in organic electrolyte solutions, J. Electroanal. Chem. 130 (1981) 221.
[26] G. Blustein, C.F. Zinola, Inhibition of steel corrosion by calcium benzoate adsorption in nitrate solutions; theoretical and experimental approach, J. Colloid Interface Sci. 278 (2004) 393.
[27] P. Kern, D. Landolt, Adsorption of organic corrosion inhibitors on iron in the active and passive state. A replacement reaction between inhibitor and water studied with the rotating quartz crystal microbalance, Electrochim. Acta 47 (2001) 589.
[28] C. Monticelli, A. Frignani, G. Trabanelli, A study on corrosion inhibitors for concrete application, Cem. Concr. Res. 30 (2000) 635.
[29] J.M. Gaidis, Chemistry of corrosion inhibitors, Cem. Concr. Compos. 26 (2004) 181.
[30] F. Galliano, D. Landolt, Evaluation of corrosion protection properties of additives for waterborne epoxy coatings on steel, Prog. Org. Coat. 44 (2002) 217.
[31] S.A. Hodges, W.M. Uphues, M.T. Tran, Non-toxic corrosion inhibitive synergistic system, Surf. Coat. Int. 4 (1997) 178.
[32] C.H. Simpson, Non-toxic, self-priming coatings for aluminium and steel, Paint Coat. Ind. (1993).
[33] M.A. Jackson, Formulation of waterborne epoxy primers: an evaluation of anticorrosive pigment, J. Protect. Coat. Lignin 7 (1990) 54.
[34] A. Kalendová, Methods for testing and evaluating the flash corrosion, Prog. Org. Coat. 44 (2002) 201.
[35] Halox® Flash-X330, Halox Flash Rust Inhibitors.
[36] G. Pollano, A. Lurier, Factors affecting salt spray resistance of an aqueous coating on metal, Paint Coat. Ind. May/June (1987) 15.
[37] I. Chet, P. Asketh, R. Mitchell, Repulsion of bacteria from marine surfaces, Appl. Microbiol. 30 (1975) 1043.
[38] M. Stupak, M. García, M. Pérez, Non-toxic alternative compounds for marine antifouling paints, Int. Biodeterior. Biodegrad. 52 (2003) 49.
[39] Z. Szklarska-Smialowska, J. Mankowsky, Cathodic inhibition of the corrosion of mild steel in phosphate, tungstate, arsenate and silicate solutions containing Ca^{2+} ions, Br. Corros. J. 4 (1969) 271.
[40] Z. Szklarska-Smialowska, R.W. Staehle, Ellipsometric study of the formation of films on iron in orthophosphate solution, J. Electrochem. Soc. 121 (1974) 1393.
[41] A. Gerhard, A. Bittner, Second generation phosphate anti-corrosive pigments. Formulating rules for full replacement of new anti-corrosive pigments, JCT 58 (1986) 59.
[42] A. Bittner, Advanced phosphate anticorrosive pigments for compliant primers, JCT 61 (1984) 114.
[43] C.A. Giúdice, J.C. Benítez, V.J.D. Rascio, Study of variables which affect dispersion of antifouling paints in ball mills, JOCCA 63 (1980) 153.
[44] S. Gee, Water borne coatings, Surf. Coat. J. 80 (1997) 316.
[45] B.A. Boukamp, Report CT88/265/128, CT89/214/128, University of Twente, The Netherlands, 1989.
[46] D.M. Santágata, P.R. Seré, C.I. Elsner, A.R. Di Sarli, Evaluation of the surface treatment effect on the corrosion performance of paint coated carbon steel, Prog. Org. Coat. 33 (1998) 44.
[47] O. Ferraz, E. Cavalcanti, A.R. Di Sarli, The characterization of protective properties for some naval steel/polymeric coatings/3%NaCl solution systems by EIS and visual assessment, Corros. Sci. 37 (1995) 1267.
[48] M.C. Deyá, Thesis. Universidad Nacional de La Plata, 2002.
[49] P.R. Seré, D.M. Santágata, C.I. Elsner, A.R. Di Sarli, The influence of the meted of application of paint on the corrosion of the substrate as asessed by ASTM and electrochemical methods, Surf. Coat. Int. 3 (1998) 128.
[50] J.V. Standish, H. Leidheiser Jr., The effect of water on the dielectric properties of a corrosion-protective epoxy polyamide coating, Org. Coat. Plast. Chem. 43 (1980) 565.
[51] C. Wilson, D. Wilson, Comprehensive Analytical Chemistry, Elsevier Publishing Company, Amsterdam, 1960.
[52] R.B. Fischer, D.G. Peters, Quantitative Chemical Analysis, W.B. Saunders Co., Mexico, 1968.
[53] G. Blustein, B. del Amo, J. Jaén, A.R. Di Sarli, R. Romagnoli, Ferric benzoate: an eco-friendly inhibitor for paints, to be published next.
[54] G. Larramona, C. Gutiérrez, The passive film on iron at pH 1–14. A potential-modulated reflectance study, J. Electrochem. Soc. 136 (1989) 2171.
[55] G. Blustein, M.C. Deyá, R. Romagnoli, B. del Amo, Three generations of inorganic phosphates in solvent and water-borne paints: a synergism case, Appl. Surf. Sci. 252 (2005) 1386.
[56] T. Szauer, Electrical and electrochemical resistance for protective non metallic coatings, Prog. Org. Coat. 10 (1982) 171.
[57] C.I. Elsner, A.R. Di Sarli, Comparison between electrochemical impedance and salt spray test in evaluating the effect of epoxy paints, J. Braz. Chem. Soc. 5 (1994) 15.
[58] H. Leidheiser, Electrical and electrochemical measurements as predictors of corrosion at the metal-organic coatings interface, Prog. Org. Coat. 7 (1979) 70.